

## RESEARCH ARTICLE

## 730 nm Light-Induced Cleavage of BODIPY Photocages via Entropy-Driven Triplet Sensitization

Jussi Isokuortti, Kaiqi Long, Zahra Gounani, Yichi Zhang, Omar Alsaedy, Weiping Wang,\*  
Timo Laaksonen,\* and Nikita A. Durandin\*

Light-activated drug delivery systems allow precise spatiotemporal control of a drug release process. However, safe and efficient drug release activation needs a low-power nonpulsed red/near-infrared light with high tissue penetration depth. Nevertheless, such systems remain a challenge. Herein, a self-assembled nanovehicle made of 2,6-diiodo-B-dimethyl-boron dipyrromethene (BODIPY)-based photocleavable trigonal molecules bearing Pt(II) meso-tetraphenyltetranaphthoporhyrin photosensitizer and a fluorescent release marker Nile Red in hydrophobic core is introduced. The system employs endothermic triplet–triplet energy transfer between the photosensitizer and the trigonal molecule, leading to the cleavage of the trigonal molecule followed by cargo release. This allows to engage 730 nm light to cleave BODIPY photoremovable protecting groups (PPGs) instead of 530 nm light that would be needed for direct photocage excitation. Therefore, the approach unleashes the desired activation of drug release via photocleavage with longer wavelengths (within the phototherapeutic window) without any chemical modification of the PPGs. Cell studies demonstrate fast intracellular uptake of the nanovehicles by PC3 human prostate cancer cells with accumulation in lysosomes in 2 h. Light irradiation at 730 nm on nanovehicles dispersed in cell media leads to payload release. Remarkably, the system exhibits higher release efficiency at low oxygen concentration than at ambient thus allowing to tackle aggressive hypoxic solid tumors.

photocatalysis, and 3D printing.<sup>[2]</sup> Photoremovable protecting groups (PPGs), such as o-nitrobenzenes,<sup>[3]</sup> coumarins,<sup>[4–6]</sup> and boron-dipyrromethenes (BODIPYs),<sup>[7]</sup> absorb UV and/or visible light followed by bond cleavage between the PPGs and the cargo molecules. However, long-wavelength light, in particular within the red/near-infrared (NIR) window (625–900 nm), is preferable for biomedical applications and additive manufacturing due to its superior tissue penetration, lower phototoxicity, and reduced scattering. Thus, the development of long-wavelength light-triggerable photocleavage reactions becomes highly desirable.

Nevertheless, longer-wavelength absorbing PPGs are inherently less photochemically efficient than the shorter-wavelength absorbing derivatives due to the lower-energy excited states that decay rapidly as dictated by the energy gap law. Many efforts in synthesizing red/NIR light-responsive PPGs with expanded  $\pi$ -conjugating area or novel chemical substitutions have resulted in unsatisfying photolytic yields and relatively low absorption coefficients. Alternative pathways,

such as multiphoton excitation<sup>[8–10]</sup> and photon upconversion,<sup>[11–13]</sup> have been explored to utilize NIR light for activating short-wavelength light-responsive PPGs. Further developments can also be seen by developing a one-photon triplet sensitization process to mimic but simplify the photon upconversion process. Particularly for BODIPYs that possess a low-lying triplet state compared to the first excited singlet and

## 1. Introduction

Photocleavage reactions, also known as photo-uncaging reactions, have emerged as a promising photochemical process enabling precise control over bond cleavage using light. They facilitate photochemical control of molecular structures and activities for diverse applications like photopharmacology,<sup>[1]</sup>

J. Isokuortti, O. Alsaedy, N. A. Durandin  
Faculty of Engineering and Natural Sciences  
Tampere University  
Tampere FI-33101, Finland  
E-mail: [nikita.durandin@tuni.fi](mailto:nikita.durandin@tuni.fi)

 The ORCID identification number(s) for the author(s) of this article can be found under <https://doi.org/10.1002/adom.202400310>

© 2024 The Author(s). Advanced Optical Materials published by Wiley-VCH GmbH. This is an open access article under the terms of the [Creative Commons Attribution](#) License, which permits use, distribution and reproduction in any medium, provided the original work is properly cited.

DOI: 10.1002/adom.202400310

K. Long, Y. Zhang, W. Wang  
Key Laboratory of Pharmaceutical Biotechnology & Dr. Li Dak-Sum  
Research Centre & Department of Pharmacology and Pharmacy  
The University of Hong Kong  
Hong Kong 999077, China  
E-mail: [wangwp@hku.hk](mailto:wangwp@hku.hk)  
Z. Gounani, T. Laaksonen  
Division of Pharmaceutical Biosciences  
Drug Research Program  
Faculty of Pharmacy  
University of Helsinki  
Helsinki FI-00014, Finland  
E-mail: [timo.laaksonen@helsinki.fi](mailto:timo.laaksonen@helsinki.fi)

the uncaging reaction can occur via this triplet state, photosensitization provides an efficient and energy-conserving pathway with increased photolytic quantum yields.<sup>[14–17]</sup>

Here, we demonstrate a photocleavage reaction via an endothermic, that is, donor energy is lower than acceptor, triplet sensitization pathway. A far-red ( $\lambda_{\text{max}} = 690 \text{ nm}$ ) light-absorbing photosensitizer, Pt(II) meso-tetraphenyltetranaphthoporphyrin (PtN), was employed in combination with (2,6-diiodo-B-dimethyl-BODIPY)<sub>3</sub>-tris(2-aminoethyl)amine, shortly BTAEA, as the energy acceptor. Often, the endothermic triplet–triplet energy transfer (TTET) process is considered thermodynamically unfavorable and thus omitted. However, endothermic TTET has been successfully employed recently for triplet fusion upconversion and photoswitching, just to name a few.<sup>[18–21]</sup> However, these examples are still limited.

Despite of endothermic nature of TTET, efficient photolysis of BTAEA was observed upon 730 nm light indicating that TTET still occurs between PtN and BTAEA. Owing to the self-assembling property of BTAEA via  $\pi$ – $\pi$  and hydrophobic interactions,<sup>[15]</sup> the hydrophobic photosensitizer can be easily solubilized upon integrating it into BTAEA-formed nanosystem and the triplet sensitization can be performed also in an aqueous environment, indicating excellent potential for biomedical applications. Moreover, in the same fashion, BTAEA can incorporate hydrophobic cargo molecules, for example, drugs without drug–PPG conjugation, making it the perfect light-responsive drug nanocarrier.

## 2. Results and Discussion

### 2.1. Nanoparticle Preparation and Characterization

Nanoparticles were fabricated using flash nanoprecipitation method followed by several rounds of centrifugation to purify them from unencapsulated dyes (for more details, see Supporting Information).<sup>[15]</sup> The obtained nanoparticles had an average diameter of ca. 90 nm (PDI < 0.2) measured by dynamic light scattering. At the same time, transmission electron microscopy revealed 86 nm size of nanovehicles (Figures S5 and S6, Supporting Information). Notably, the nanoparticles were stable for at least 2 months.

Encapsulation of the dyes into the nanoparticles was confirmed utilizing UV–vis spectrophotometry (Figure S7, Supporting Information). Significantly, these feeding ratios yielded 100% encapsulation efficiency for the Nile Red fluorescent release indicator while for BTAEA and PtN the values were 39% and 18%, respectively. This resulted in 11.8 BTAEA/PtN molar ratio, ensuring that every nanoparticle contained the triplet photosensitizer in its hydrophobic core.

### 2.2. Probing the Character of Triplet–Triplet Energy Transfer

In order to study the kinetics of TTET, we employed 2,6-diiodo-B-dimethyl-BODIPY-OH, a chromophoric analog of the trigonal molecule BTAEA, for TTET experiments in solutions. This allows to neglect the size effect of BTAEA on the diffusion rate constant. For these experiments, the PtN photosensitizer and 2,6-diiodo-B-dimethyl-BODIPY-OH molecules (BODIPY-OH) were dissolved in degassed dimethyl sulfoxide (DMSO) with the addition

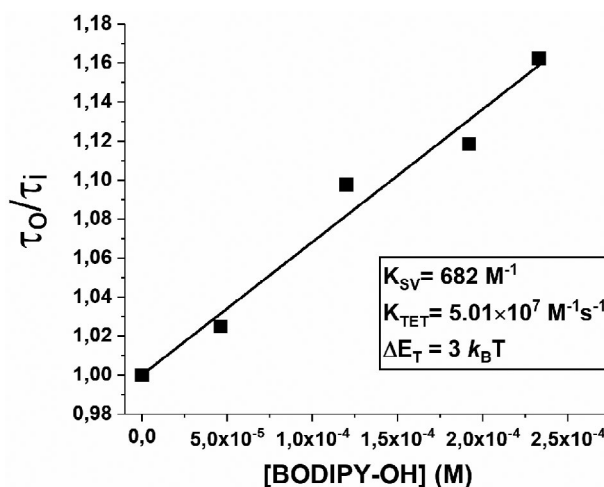


**Figure 1.** Phosphorescence quenching results of PtN by 2,6-diiodo-B-dimethyl-BODIPY-OH (BODIPY-OH) as Stern–Volmer plot with linear fit for Stern–Volmer constants ( $K_{\text{SV}}$ ), rate constants of triplet energy transfer ( $k_{\text{TTET}}$ ) and triplet energy gap ( $\Delta E_{\text{T}}$ ).

of bis(methylthio)methane serving as an oxygen scavenger.<sup>[22]</sup> TTET was monitored by measuring PtN phosphorescence lifetime in presence of various 2,6-diiodo-B-dimethyl-BODIPY-OH concentrations (Figures S3 and S4, Supporting Information). The resulting Stern–Volmer plot is shown in **Figure 1**. The Stern–Volmer quenching constant ( $K_{\text{SV}}$ ) was further used to calculate the TTET rate constant ( $k_{\text{TTET}}$ ):

$$\frac{\tau_0}{\tau_i} = 1 + K_{\text{SV}} \times [2,6\text{-diiodo-B-dimethyl-BODIPY-OH}] \quad (1)$$

$$k_{\text{TTET}} = \frac{K_{\text{SV}}}{\tau_0} \quad (2)$$

where  $\tau_0$  is the unquenched phosphorescence lifetime of the photosensitizer, that is, 13.6  $\mu\text{s}$ . The quenching study yielded a  $k_{\text{TTET}}$  of  $5.01 \times 10^7 \text{ M}^{-1} \text{ s}^{-1}$ , which is 20 times slower than  $k_{\text{diff}}$ . This TTET rate constant value was then employed to evaluate the triplet energy gap ( $\Delta E_{\text{T}}$ ) between the PtN and 2,6-diiodo-B-dimethyl-BODIPY-OH triplet states:<sup>[23]</sup>

$$\frac{\Delta E_{\text{T}}}{k_{\text{B}} T} = \ln \left( \frac{k_{\text{diff}}}{k_{\text{TTET}}} - 1 \right) \quad (3)$$

where  $k_{\text{B}}$  is the Boltzmann constant,  $T$  is the temperature, and  $k_{\text{diff}} = 1.1 \times 10^9 \text{ M}^{-1} \text{ s}^{-1}$  is the diffusion rate constant in DMSO (see Supporting Information).<sup>[19]</sup> The calculated  $3 k_{\text{B}} T$  (or 0.078 eV) triplet energy gap reveals that TTET is substantially endothermic. Based on the estimated energy gap and the triplet energy of PtN obtained from the phosphorescence spectrum (1.39 eV, Figure S2, Supporting Information), we calculated the triplet energy of 2,6-diiodo-B-dimethyl-BODIPY-OH as 1.47 eV. This value is in good agreement with TD-DFT calculated one (1.52 eV).<sup>[14,15]</sup> Altogether, the quenching results indicate that TTET occurs between the PtN photosensitizer and the 2,6-diiodo-B-dimethyl-BODIPY-OH acceptor even through a considerably endothermic energy gap.

### 2.3. Co-Localized Triplet Energy Transfer Followed by Photocleavage

To investigate whether endothermic TTET between PtN and BTAEA can lead to photocleavage and consequently cargo release, the nanoparticles were irradiated with 730 nm light. Since triplets are inherently oxygen-sensitive, we expected to have negligible or substantially smaller BTAEA photocleavage upon excitation of PtN at ambient versus hypoxia.

Photocleavage was investigated by using high-performance liquid chromatography (HPLC) with UV-vis detection (Figures S8–S10, Supporting Information). For this set of experiments, the nanoparticles encapsulated only PtN. Before the analysis, the nanoparticle samples were left intact or treated with ca. 25 mM sodium sulfite, a potent ground state oxygen scavenger,<sup>[24]</sup> to create hypoxic conditions and then illuminated with 730 nm LED. At ambient, 16% of BTAEA was photolyzed in 5 min under 730 nm light illumination ( $170 \text{ mW cm}^{-2}$ , see Figure 2). At the same time at hypoxic conditions, 42% photocleavage was achieved using the same light dosage. A 20-min exposure time led to ca. 76% cleavage efficiency at hypoxic conditions. BTAEA nanoparticles without the PtN photosensitizer did not show any photocleavage after the same illumination period, regardless of oxygen status.

To demonstrate that the BTAEA photocleavage results in a cargo release from the nanoparticles, we employed a hydrophobic fluorescent reporter molecule Nile Red (Scheme 1). Nile Red has a high fluorescence quantum yield when it is dissolved in an organic solvent such as THF, DMF, or when it is incorporated into hydrophobic compartments of proteins or nanoparticles.<sup>[25–27]</sup> Once it is introduced to an aqueous solution it aggregates and loses its emission properties.<sup>[15]</sup> The absorption spectrum of Nile Red allows selective excitation of the dye at 580 nm for release studies without exciting either the PtN photosensitizer or the BTAEA photocage (Figure S1, Supporting Information).

After just 2 min of light irradiation (730 nm,  $170 \text{ mW cm}^{-2}$ ), 22% of Nile Red was released at hypoxic conditions (Figure S11, Supporting Information). This was anticipated considering the efficient BTAEA photocleavage verified by HPLC (vide supra). Further light exposure led to even more release, reaching ca. 38% in 25 min. In order to make release faster, we increased power density up to  $870 \text{ mW cm}^{-2}$  and checked the release profile of the cargo molecule from the nanoparticles. Indeed, the higher power density of excitation light resulted in more efficient release within the same 25-min period of time, that is, 52%. The release was accompanied with a decrease in the size of nanoparticles (71 nm versus initial 86 nm) due to the cleavage of BTAEA followed by a partial degradation of the BODIPY-OH. Little to no release was observed at ambient conditions despite even higher power density ( $870 \text{ mW cm}^{-2}$ ) used for these experiments (Figure 2).

### 2.4. On the Mechanism of Photocleavage via Endothermic Energy Transfer

Although there are ongoing debates about the precise photorelease mechanism from BODIPY photocages, there are indications that it is a photo- $\text{SN}_1$ -type mechanism based on ionization-dissociation heterolysis.<sup>[28]</sup> Importantly, BODIPY-based photocages can undergo photocleavage involving a triplet mani-

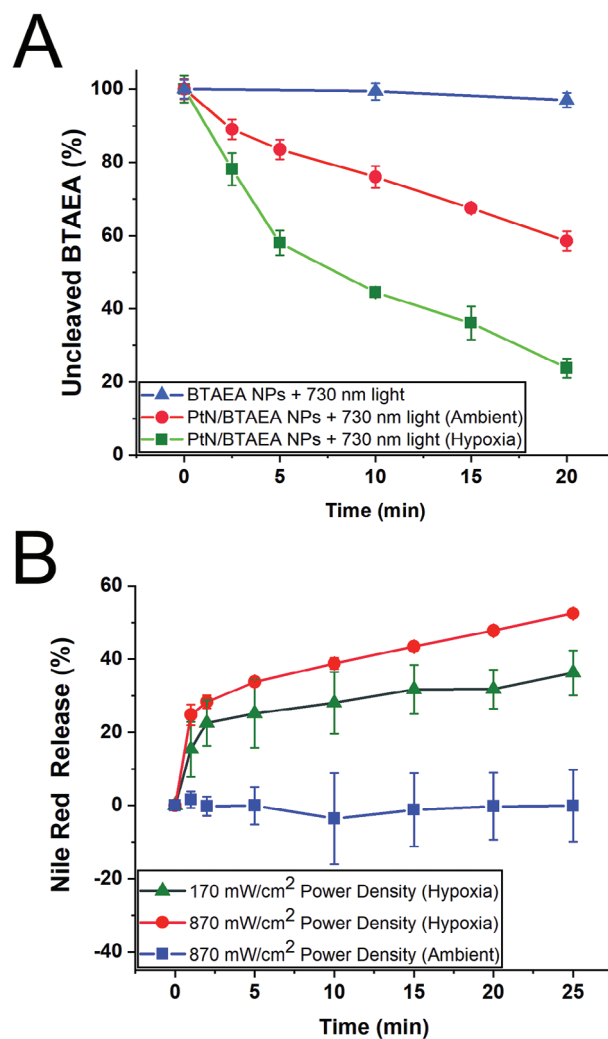
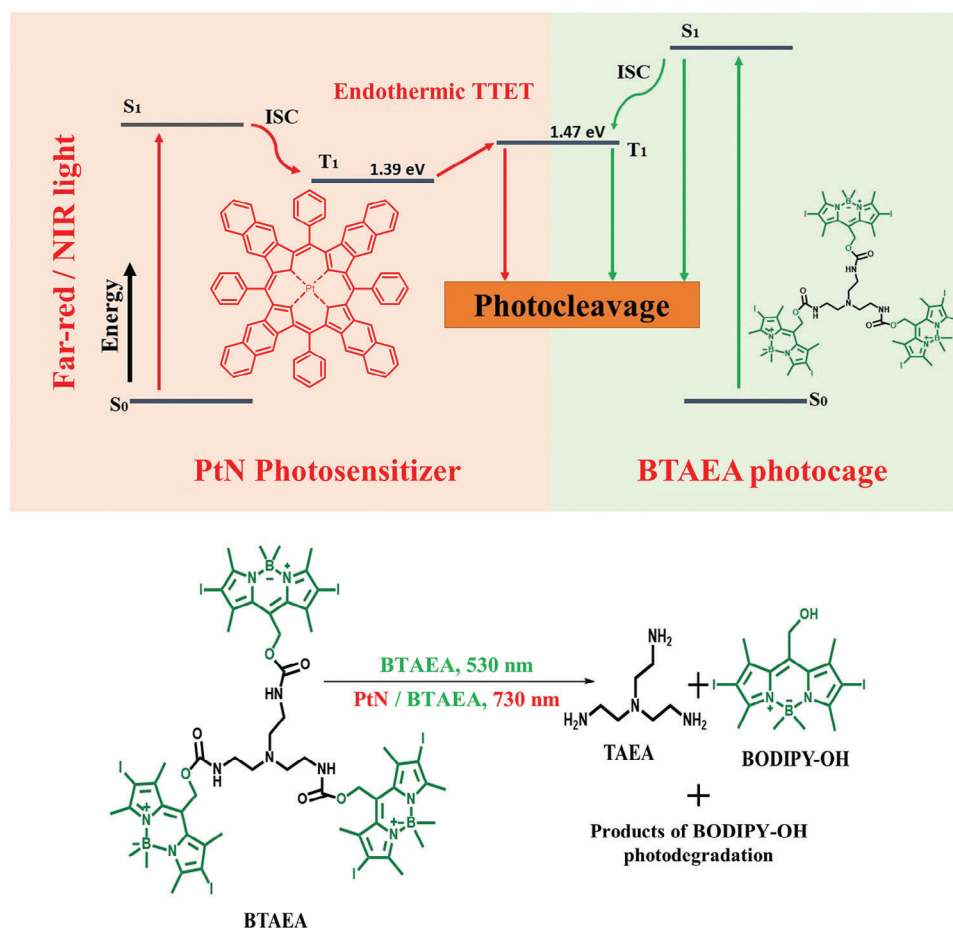


**Figure 2.** A) Dependence of BTAEA photocleavage in nanoparticles upon 730 nm illumination ( $170 \text{ mW cm}^{-2}$ ) in the presence or absence of PtN photosensitizer and normoxia versus hypoxia conditions monitored using HPLC. B) Release profile of Nile Red from nanoparticles upon 730 nm light irradiation varying power density at ambient versus hypoxia conditions ( $n = 3$ ). “NPs” shown in (A) refers to nanoparticles.

fold once their triplet state is populated either via intersystem crossing or triplet-triplet energy transfer.<sup>[29]</sup> Based on our experimental data, TTET between PtN and 2,6-diiodo-B-dimethyl BODIPY-OH and thus BTAEA is highly endothermic with  $3 k_B T$  triplet energy gap between triplet state of the photosensitizer (donor) and the BODIPY moiety acceptor. Therefore, no photocleavage could be expected due to hindered TTET from PtN to the 2,6-diiodo-B-dimethyl-BODIPY moieties and orders of magnitude more rapid exothermic reverse TTET (rTTET) from the acceptor to the photosensitizer.<sup>[23]</sup> Despite the seemingly unfavorable thermodynamics of TTET, photocleavage was still observed in our experiments (vide supra). We postulate that the reasonably long triplet state lifetime of PtN photosensitizer ( $13.6 \mu\text{s}$ ) and high local concentration of the BODIPY acceptor moieties in the nanoparticle facilitate the process of TTET. Indeed, our



**Scheme 1.** Upper panel: The Jablonski diagram of the BTAEA photocleavage. The left section (red one) represents the triplet-sensitized mechanism of BTAEA photocleavage upon 730 nm light excitation employing PtN photosensitizer. The right one (green panel) shows photocleavage using direct excitation of BTAEA chromophore with green, for example, 530 nm light. Lower Panel: Reaction scheme of BTAEA photocleavage.

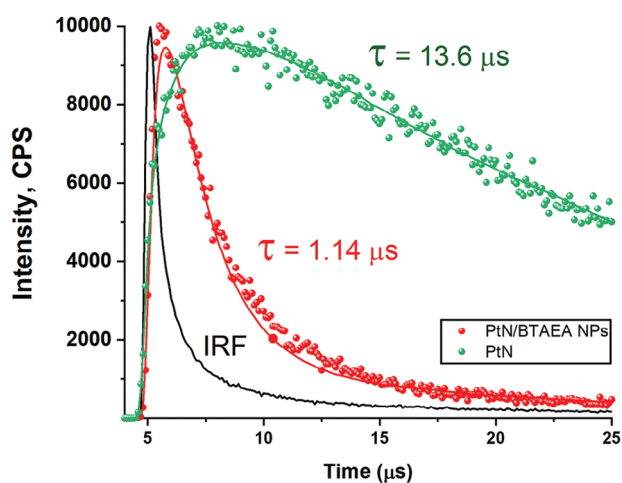


**Figure 3.** Time-resolved phosphorescence decays of PtN ( $\lambda_{\text{exc}} = 690 \text{ nm}$ ,  $\lambda_{\text{em}} = 895 \text{ nm}$ ) in DMSO or PtN/BTAEA nanoparticles (samples were deoxygenated). Scatter plots represent raw data, bold lines are reconvolution fittings.

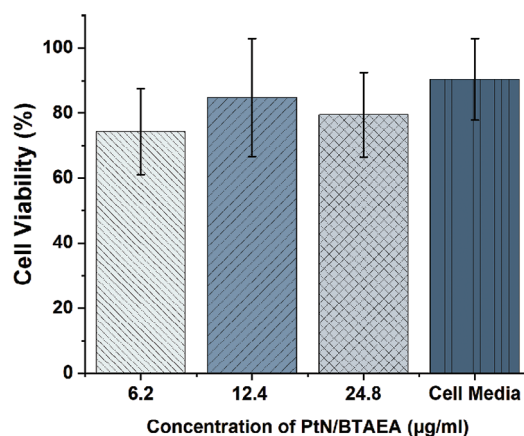


**Figure 4.** The relative viability of PC3 cells cultured 24 h before treatment with PtN/BTAEA nanoparticles for 2 h at three concentrations of 6.2, 12.4, and 24.8  $\mu\text{g mL}^{-1}$  (BTAEA concentration is mentioned). The graph presents the cell viabilities assessed with alamarBlue assay (mean  $\pm$  SD,  $n = 4$ ). "PtN/BTAEA" shown in the figure refers to PtN/BTAEA nanoparticles.



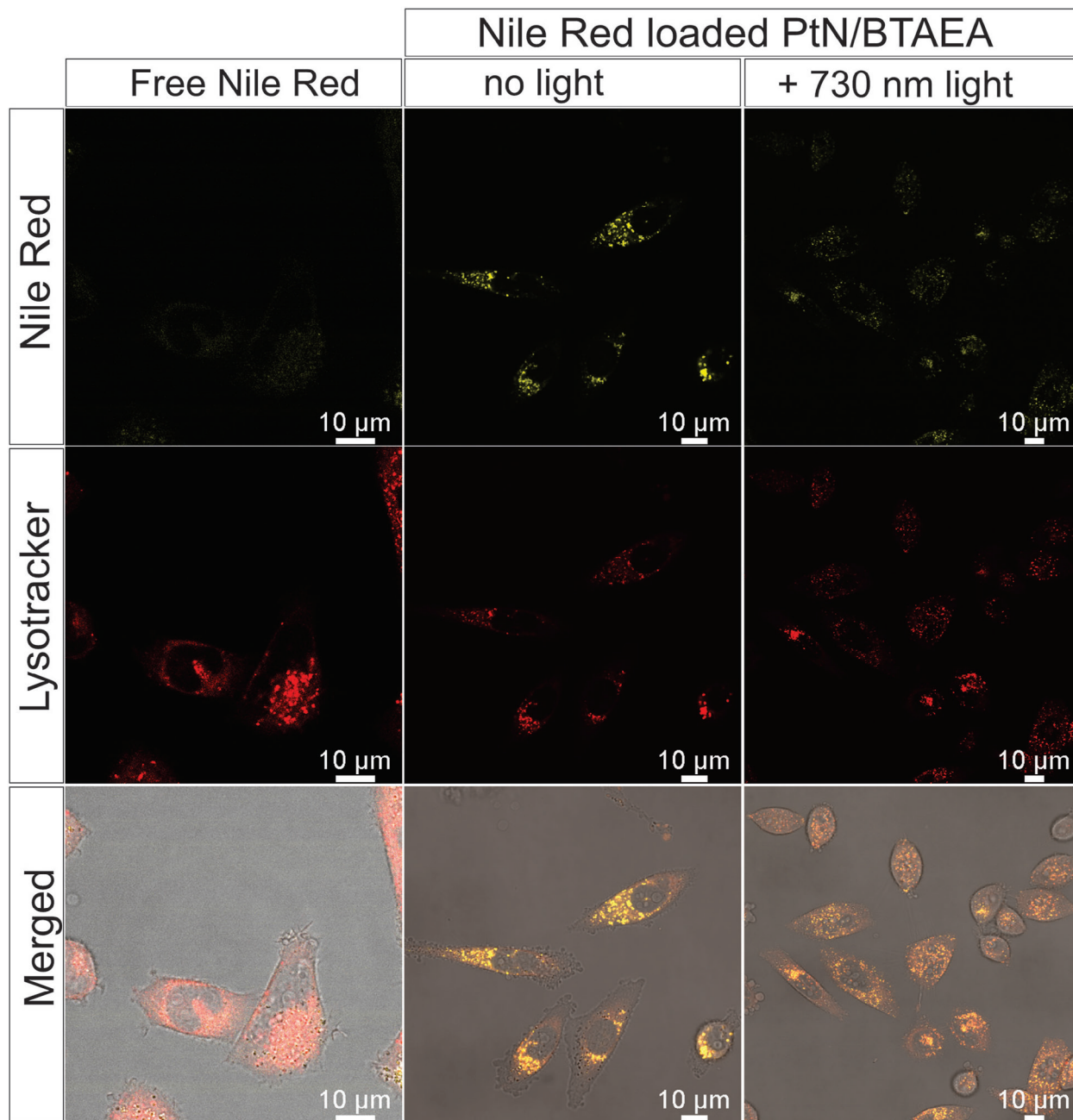


**Figure 5.** In vitro assessment of the light-triggered cargo release. CLSM images of PC3 cells incubated with free Nile Red (prepared in water), and PtN/BTAEA with or without 730 nm light irradiation. Light-irradiated PtN/BTAEA nanoparticles and free Nile Red showed lowest fluorescent intensity indicating the release of Nile Red from PtN/BTAEA upon 730 nm light exposure. “PtN/BTAEA” shown in the figure refers to PtN/BTAEA nanoparticles.

phosphorescence studies of PtN/BTAEA nanoparticles revealed substantial quenching of PtN triplet state lifetime, that is, down to 1.14  $\mu$ s (Figure 3). This leads to  $\Phi_{\text{TTET}}$  being almost 92%.

We attribute this result to the considerable entropy factor involved in the TTET process:<sup>[18–21,30]</sup>

$$\Delta S = k_B \ln \left( \frac{[\text{BTAEA}] [\text{PtN}^*]}{[\text{PtN}] [\text{BTAEA}^*]} \right) \quad (4)$$

The triplet lifetime of 2,6-diiodo-BODIPY photocages is in the order of 120 ns,<sup>[31]</sup> apparently, due to fast charge separation followed by dissociation of the cage into BODIPY carbocation with low energy. This fact leads to reduced concentration of BODIPY triplet states capable to perform rTTET,<sup>[18]</sup> which, in turn, diminishes the dominator of Equation (4) resulting in a large entropy gain. This makes overall process of TTET from PtN to BTAEA followed by photocleavage inside nanoparticles more feasible. Altogether, it leads to modest triplet-sensitized photocleavage

quantum yields of 0.195% and 0.098% at hypoxia and normoxia, respectively (see Supporting Information).

## 2.5. Cellular Uptake, Viability, and Cargo Release

The dark cytotoxicity of PtN/BTAEA nanoparticles was tested against PC3 human prostate cancer cells. The results did not indicate any significant toxicity of the nanoparticles up to  $24.8 \mu\text{g mL}^{-1}$  of BTAEA compared to control cells that were grown in cell growth media (Figure 4).

The uptake and trafficking of PtN/BTAEA nanoparticles in PC3 cells were monitored by loading the nanoparticles with Nile Red as a fluorescence marker. LysoTracker Deep Red was used to visualize PC3 lysosomes to check the co-localization of the nanoparticles and dye in the cells (Figure 5). Efficient uptake of PtN/BTAEA nanoparticles and further co-localization in lysosomes after 2 h was confirmed by Confocal Laser Scanning Microscopy (CLSM). The light-triggered cargo release was evaluated by using PtN/BTAEA ( $24.8 \mu\text{g mL}^{-1}$ ) nanoparticles loaded with Nile Red in cell media while exposing them to 730 nm light ( $870 \text{ mW cm}^{-2}$ ) for 30 min at ambient before adding to cells. Cell distribution and fluorescent intensity of free Nile Red prepared in water was used as a reference for Nile Red released from PtN/BTAEA nanoparticles after 730 nm light exposure.

As the PtN/BTAEA nanoparticles provide a lipophilic environment for Nile Red, intact nanocarriers produced higher probe fluorescence signal compared to those that had released their cargo. Figure 5 clearly shows that light-treated PtN/BTAEA nanoparticles possess lower Nile Red fluorescent intensity than nonirradiated ones and their fluorescence signal is comparable with free Nile Red. These results demonstrate that a payload of PtN/BTAEA nanoparticles can be released upon 730 nm light irradiation.

## 3. Conclusion

We developed a light-triggered drug delivery system activated by 730 nm light with good performance at hypoxic conditions. This combination of properties is rarely achieved, making our system stand out from other conventional light-based therapies including photodynamic therapy and/or reactive oxygen species-dependent drug release systems. In our work, the system relies on endothermic TTET between the PtN photosensitizer and the photocleavable BODIPY-based self-assembling molecule to induce a cargo release. Harnessing entropy to facilitate the process makes overall TTET efficient enough to indirectly excite the photoprotecting group. Thus, utilization of PtN photosensitizer as a far-red light absorbing antenna together with endothermic TTET<sup>[19–21]</sup> allow to further expand excitation wavelength range for BODIPY PPGs (usually absorbing 530 nm green light) to a wavelength even 200 nm longer without running a new synthesis. We envisage that the approach based on endothermic TTET is versatile and can be applicable for many other PPGs beyond the BODIPY chromophore<sup>[32–35]</sup> for benefits in controlled drug delivery. Moreover, the photocleavage and, consequently, the cargo release were substantially higher at hypoxia than normoxia, which can project further utilization of the approach to selectively target hypoxic solid tumours without affecting healthy normoxic tissues.

## Supporting Information

Supporting Information is available from the Wiley Online Library or from the author.

## Acknowledgements

The authors gratefully acknowledge financial support from the Academy of Finland (Grant No. 316893 and No. 354792, PREIN Flagship program, No. 320165), the European Research Council (ERC Consolidator Grant Project PADRE, decision number 101001016), and the National Natural Science Foundation of China (Excellent Young Scientists Fund, No. 82222903).

## Conflict of Interest

The authors declare no conflict of interest.

## Data Availability Statement

The data that support the findings of this study are available from the corresponding author upon reasonable request.

## Keywords

BODIPY, drug release, endothermic, energy transfer, photocleavage

Received: February 1, 2024  
Revised: May 15, 2024  
Published online: July 5, 2024

- [1] J. Liu, W. Kang, W. Wang, *Photochem. Photobiol.* **2022**, 98, 288.
- [2] R. Batchelor, T. Messer, M. Hippler, M. Wegener, C. Barner-Kowollik, E. Blasco, *Adv. Mater.* **2019**, 31, 1904085.
- [3] C. W. Wright, Z.-F. Guo, F.-S. Liang, *ChemBioChem* **2015**, 16, 254.
- [4] K. Long, Y. Yang, W. Lv, K. Jiang, Y. Li, A. C. Y. Lo, W. C. Lam, C. Zhan, W. Wang, *Adv. Sci.* **2021**, 8, 2101754.
- [5] T. Wang, K. Long, Y. Zhou, X. Jiang, J. Liu, J. H. C. Fong, A. S. L. Wong, W.-L. Ng, W. Wang, *ACS Pharmacol. Transl. Sci.* **2022**, 5, 149.
- [6] Y. Liu, K. Long, W. Kang, T. Wang, W. Wang, *Adv. Nanobiomed Res* **2022**, 2, 2200017.
- [7] P. K. Singh, P. Majumdar, S. P. Singh, *Coord. Chem. Rev.* **2021**, 449, 214193.
- [8] C. A. Hammer, K. Falahati, A. Jakob, R. Klimek, I. Burghardt, A. Heckel, J. Wachtveitl, *J. Phys. Chem. Lett.* **2018**, 9, 1448.
- [9] M. Klausen, M. Blanchard-Desce, J. Photochem. Photobiol. C: Photochem. Rev. **2021**, 48, 100423.
- [10] S. Piant, F. Bolze, A. Specht, *Opt. Mater. Express* **2016**, 6, 1679.
- [11] S. H. C. Askes, A. Bahreman, S. Bonnet, *Angew. Chem., Int. Ed.* **2014**, 53, 1029.
- [12] W. Wang, Q. Liu, C. Zhan, A. Barhoumi, T. Yang, R. G. Wylie, P. A. Armstrong, D. S. Kohane, *Nano Lett.* **2015**, 15, 6332.
- [13] A. Bagheri, H. Arandiyani, C. Boyer, M. Lim, *Adv. Sci.* **2016**, 3, 1500437.
- [14] W. Lv, Y. Li, F. Li, X. Lan, Y. Zhang, L. Du, Q. Zhao, D. L. Phillips, W. Wang, *J. Am. Chem. Soc.* **2019**, 141, 17482.
- [15] K. Long, H. Han, W. Kang, W. Lv, L. Wang, Y. Wang, L. Ge, W. Wang, *J. Nanobiotechnol.* **2021**, 19, 357.
- [16] W. Lv, K. Long, Y. Yang, S. Chen, C. Zhan, W. Wang, *Adv. Healthcare Mater.* **2020**, 9, 2001118.

- [17] Long, K., Lv, W., Wang, Z., Zhang, Y., Chen, K., Fan, N., Li, F., Zhang, Y., Wang, W., *Nat. Commun.* **2023**, *14*, 8112.
- [18] Y. Y. Cheng, B. Fückel, T. Khoury, R. G. C. R. Clady, N. J. Ekins-Daukes, M. J. Crossley, T. W. Schmidt, *J. Phys. Chem. A* **2011**, *115*, 1047.
- [19] J. Isokuortti, K. Kuntze, M. Virkki, Z. Ahmed, E. Vuorimaa-Laukkanen, M. A. Filatov, A. Turshatov, T. Laaksonen, A. Priimagi, N. A. Durandin, *Chem. Sci.* **2021**, *12*, 7504.
- [20] J. Isokuortti, S. R. Allu, A. Efimov, E. Vuorimaa-Laukkanen, N. V. Tkachenko, S. A. Vinogradov, T. Laaksonen, N. A. Durandin, *J. Phys. Chem. Lett.* **2020**, *11*, 318.
- [21] J. Isokuortti, T. Griebenow, J.-S. von Glasenapp, T. Raeker, M. A. Filatov, T. Laaksonen, R. Herges, N. A. Durandin, *Chem. Sci.* **2023**, *14*, 9161.
- [22] D. Dzebo, K. Moth-Poulsen, B. Albinsson, *Photochem. Photobiol. Sci.* **2017**, *16*, 1327.
- [23] K. Sandros, *Acta Chem. Scand.* **1964**, *18*, 2355.
- [24] J. Isokuortti, I. Kiiski, T. Sikanen, N. Durandin, T. Laaksonen, *J. Mater. Chem. C* **2022**, *10*, 4871.
- [25] A. K. Dutta, K. Kamada, K. Ohta, *J. Photochem. Photobiol.* **1996**, *93*, 57.
- [26] N. Ghoneim, *Spectrochim. Acta A Mol. Biomol.* **2000**, *56*, 1003.
- [27] D. L. Sackett, J. Wolff, *Anal. Biochem.* **1987**, *167*, 228.
- [28] P. Shrestha, D. Kand, R. Weinstain, A. H. Winter, *J. Am. Chem. Soc.* **2023**, *145*, 17497.
- [29] P. Shrestha, K. C. Dissanayake, E. J. Gehrmann, C. S. Wijesooriya, A. Mukhopadhyay, E. A. Smith, A. H. Winter, *J. Am. Chem. Soc.* **2020**, *142*, 15505.
- [30] N. A. Durandin, J. Isokuortti, A. Efimov, E. Vuorimaa-Laukkanen, N. V. Tkachenko, T. Laaksonen, *J. Phys. Chem. C* **2019**, *123*, 22865.
- [31] T. Slanina, P. Shrestha, E. Palao, D. Kand, J. A. Peterson, A. S. Dutton, N. Rubinstein, R. Weinstain, A. H. Winter, P. Klán, *J. Am. Chem. Soc.* **2017**, *139*, 15168.
- [32] D. Wöll, S. Walbert, K.-P. Stengele, T. J. Albert, T. Richmond, J. Norton, M. Singer, R. D. Green, W. Pfeleiderer, U. E. Steiner, *Helv. Chim. Acta* **2004**, *87*, 28.
- [33] D. Wöll, N. Lukzen, U. E. Steiner, *Photochem. Photobiol. Sci.* **2012**, *11*, 533.
- [34] S. H. C. Askes, G. U. Reddy, R. Wyrwa, S. Bonnet, *J. Am. Chem. Soc.* **2017**, *139*, 15292.
- [35] A. Fraix, C. Parisi, G. Longobardi, C. Conte, A. Pastore, M. Stornaiuolo, A. C. E. Graziano, M. E. Alberto, A. Francés-Monerris, F. Quaglia, S. Sortino, *Biomacromolecules* **2023**, *24*, 3887.